

# A Simple Parametric Classification Baseline for Generalized Category Discovery

Xin Wen<sup>1\*</sup> Bingchen Zhao<sup>2\*</sup> Xiaojuan Qi<sup>1</sup>  
<sup>1</sup>The University of Hong Kong <sup>2</sup>University of Edinburgh  
 {wenxin, xjq}@eee.hku.hk bingchen.zhao@ed.ac.uk

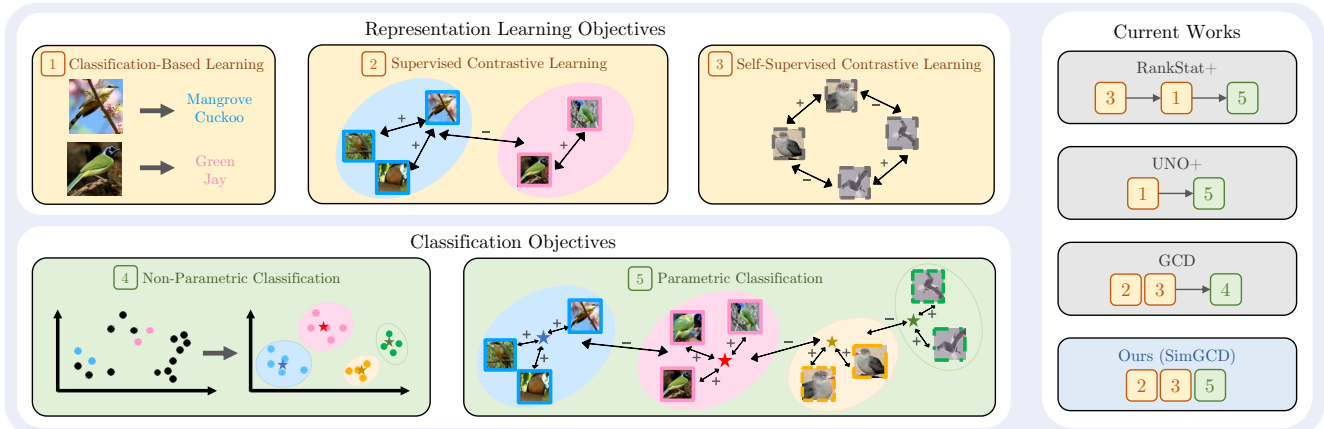


Figure 1. Left: building blocks for representation learning or classifier learning; Right: overall abstraction of current works, in which ‘→’ separates different stages of the framework. Our method builds on GCD [33], and jointly trains a parametric classifier.

## Abstract

Generalized category discovery (GCD) is a problem setting where the goal is to discover novel categories within an unlabelled dataset using the knowledge learned from a set of labelled samples. Recent works in GCD argue that a non-parametric classifier formed using semi-supervised  $k$ -means can outperform strong baselines which use parametric classifiers as it can alleviate the over-fitting to seen categories in the labelled set. In this paper, we revisit the reason that makes previous parametric classifiers fail to recognise new classes for GCD. By investigating the design choices of parametric classifiers from the perspective of model architecture, representation learning, and classifier learning, we conclude that the less discriminative representations and unreliable pseudo-labelling strategy are key factors that make parametric classifiers lag behind non-parametric ones. Motivated by our investigation, we present a simple yet effective parametric classification baseline that outperforms the previous best methods by a large margin on multiple popular GCD benchmarks. We hope the investigations and the simple baseline can serve as a cornerstone to facilitate future studies. Our code is available at: <https://github.com/CVMI-Lab/SimGCD>.

\*Equal contribution.

## 1. Introduction

With large-scale labelled datasets, deep learning methods can surpass humans in recognising images [20]. However, it is not always possible to collect large-scale human annotations for training deep learning models. Therefore, there is a rich body of recognition models that focus on learning with a large number of unlabelled data. Among them, semi-supervised learning (SSL) [3, 26, 28] is regarded as a promising approach, yet with the assumption that labelled instances are provided for each of the categories the model needs to classify. Generalized category discovery (GCD) [33] is recently formalised to relax this assumption by assuming the unlabelled data can also contain similar yet distinct categories from the labelled data. The goal of GCD is to learn a model that is able to classify the already-seen categories in the labelled data, and more importantly, jointly discover the new categories in the unlabelled data and make correct classifications. Developing a strong method for this problem could help us better utilise the easily available large-scale unlabelled datasets.

Previous works [4, 14, 17, 33] approach this problem from two perspectives: learning generic feature representations to facilitate the discovery of novel categories and generating pseudo clusters/labels for unlabelled data to guide the

learning of a classifier. The former is often achieved by using self-supervised learning methods [7, 15, 17, 19, 40, 41] to improve the generalization ability of features to novel categories. For constructing the classifier, earlier works [4, 14, 17, 40, 43] adopt a parametric approach that builds a learnable classifier on top of the extracted features. The classifier is jointly optimised with the backbone using labelled data and pseudo-labelled data.

However, recent research shows [13, 33] that parametric classifiers are prone to overfit to seen categories and thus promote the use of a non-parametric classifier such as  $k$ -means clustering. Albeit obtaining promising results, the non-parametric classifiers suffer from heavy computation costs on large-scale datasets due to the quadratic complexity of the clustering algorithm. For instance, it takes up to 3 hours to obtain a result on the Herbarium 19 dataset [29] with  $\sim 30k$  images. Besides, unlike a learnable parametric classifier, the non-parametric approach loses the ability to jointly optimise the separating hyperplane of all categories in a learnable manner, potentially being sub-optimal.

This motivates us to revisit the reason that makes previous parametric classifiers fail to recognise new classes for GCD. In a series of investigations (Sec. 3), we find that both the design of prototypical classifiers and the joint representation-classifier training paradigm are not to blame, and the misuse of representations and the unreliable pseudo-labelling strategy contribute to previous methods’ degraded performance. Based on these findings, we thus present a simple parametric classification baseline for generalized category discovery (see Figs. 1 and 7). The representation learning objective follows GCD [33], and the classification objective is simply cross-entropy for labelled samples and self-distillation [1, 7] for unlabelled samples.

The baseline is simple, yet strong, leading to around 10 points’ gains in new class accuracy on both generic image recognition datasets (*e.g.*, CIFAR100 [23]) and the fine-grained Semantic Shift Benchmark [34] over current SOTAs. Benefiting from the nature of parametric classifiers in faster label assignment, the label assignment speed dominates non-parametric classifiers (see Fig. 2).

Our contributions are summarised as follows: (1) We revisit the design choices of parametric classification and conclude the key factors that make it fail for GCD. (2) Based on the analysis, we propose a simple yet effective parametric classification baseline. (3) Our method achieves SOTA on multiple popular GCD benchmarks, challenging the recent promotion of non-parametric classification for this task.

## 2. Related Works

**Semi-Supervised Learning (SSL)** has been an important research topic where a number of methods have been proposed [3, 28, 30]. SSL assumes that the labelled instances

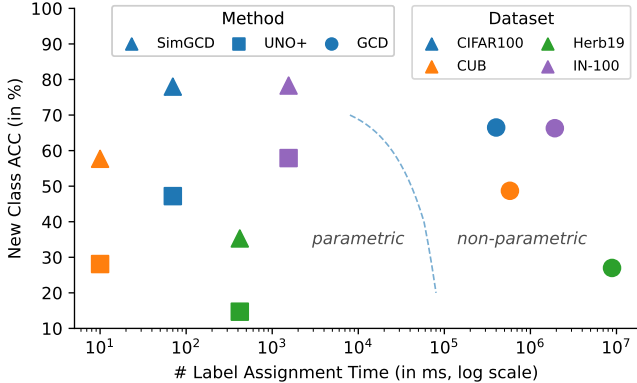


Figure 2. Comparisons with representative methods in terms of new class clustering accuracy and label assignment time cost (including post-training clustering time and inference time). Our method (SimGCD) achieves top performance in both metrics.

are available for all possible categories in the unlabelled dataset; the objective is to learn a model to perform classification using both the labelled samples as well as the large-scale available unlabelled data. One of the most effective methods for SSL is the consistency-based method, where the model is forced to learn consistent representations of two different augmentations of the same image [3, 28, 30]. Furthermore, it is also shown that self-supervised representation learning is helpful for the task of SSL [27, 39] as it can provide a strong representation for the task.

**Generalized Category Discovery (GCD)** is a relatively new problem recently formalised in Vaze *et al.* [33]. Different from the common assumption of SSL [26], GCD does not assume the unlabelled dataset comes from the same class set as the labelled dataset, posing a greater challenge for designing an effective model. GCD can be seen as a natural extension of the novel category discovery (NCD) problem [18] where it is assumed that the unlabelled dataset and the labelled dataset do not have any class overlap, thus baselines for NCD [14, 17, 40, 42, 43] can be adopted for the GCD problem by extending the classification head to have more outputs [33]. It is pointed out in [33] that a non-parametric classifier formed using semi-supervised  $k$ -means can outperform strong parametric classification baselines from NCD [14, 17] because it can alleviate the overfitting to seen categories in the labelled set. In this paper, we revisit this claim and show that parametric classifiers can reach stronger performance than non-parametric classifiers.

**Deep Clustering** aims at learning a set of semantic prototypes from unlabelled images with deep neural networks. Considering that no label information is available, the focus is on how to obtain reliable pseudo-labels. While early attempts rely on hard labels produced by  $k$ -means [5], there has been a shift towards soft labels produced by optimal transport [6, 38], and more recently sharpened predictions from an exponential moving average-updated teacher

model [1, 7]. Deep clustering has shown strong potential for unsupervised representation learning [1, 5–7, 38], unsupervised semantic segmentation [9, 37], semi-supervised learning [2], and novel category discovery [14]. In this work, we explore the techniques that make strong parametric classifiers for GCD with inspirations from deep clustering.

### 3. What Makes Parametric Classification Fail?

In this section, in order to explore the reason that makes previous parametric classifiers fail to recognise new classes for generalized category discovery, we study four perspectives: classifier architecture (Sec. 3.2), the representation it builds on (Sec. 3.3), the training paradigm and pseudo-labelling strategy (Sec. 3.4). We conclude that: both the design of prototypical classifiers and the joint representation-classifier training paradigm adopted in previous methods are not to blame, and the misuse of representations and the unreliable pseudo-labelling strategy are keys to parametric classifiers’ degraded performance. This is then verified in later ablation studies (Sec. 5.3) and leads to a state-of-the-art parametric classifier for generalized category discovery.

#### 3.1. Investigation Setting

**Generalized Category Discovery.** Given an unlabelled dataset  $\mathcal{D}^u = \{(\mathbf{x}_i^u, y_i^u)\} \in \mathcal{X} \times \mathcal{Y}_u$  where  $\mathcal{Y}_u$  is the label space of the unlabelled samples, the goal of GCD is to learn a model to categorise the samples in  $\mathcal{D}^u$  using the knowledge from a labelled dataset  $\mathcal{D}^l = \{(\mathbf{x}_i^l, y_i^l)\} \in \mathcal{X} \times \mathcal{Y}_l$  where  $\mathcal{Y}_l$  is the label space of labelled samples and  $\mathcal{Y}_l \in \mathcal{Y}_u$ . We denote the number of categories in  $\mathcal{Y}_u$  as  $K_u = |\mathcal{Y}_u|$ , it is common to assume the number of categories is known *a-priori* [14, 17, 40, 43], or can be estimated using off-the-shelf methods [18, 33].

**Representation Learning.** For representation learning, we follow GCD [33], which applies supervised contrastive learning [21] on labelled samples, and self-supervised contrastive learning [8] on all samples (detailed in Sec. 4.1).

**Classifiers.** We study two types of parametric classifiers: the *linear classifier* and the *prototypical classifier*. Considering  $f(\mathbf{x})$  as the feature vector of an image  $\mathbf{x}$  extracted using from the backbone  $f$ , the procedure for producing logits is  $\mathbf{l} = \mathbf{w}^\top f(\mathbf{x}) + \mathbf{b}$  for a *linear classifier* parameterised by  $\mathbf{w}$  and  $\mathbf{b}$ , and  $\mathbf{l} = \frac{1}{\tau}(\mathbf{w}/\|\mathbf{w}\|)^\top (f(\mathbf{x})/\|f(\mathbf{x})\|)$  for a *prototypical classifier*. Here  $1/\tau$  is a factor that scales up the norm of  $\mathbf{l}$  and facilitates optimisation of the cross-entropy loss [36]. The major difference between the two classifiers is that the latter has no bias term, and both the weight and the feature are normalised. Therefore, it can be interpreted as a set of learnable prototypes in the same space with the features, and  $\mathbf{l}$  is the scaled cosine similarity between them. Besides that, we also adopt a *mean classifier*, which denotes the  $\ell_2$ -normalised class-mean prototypes produced from the

feature of all samples, and use it to estimate the upper bound of  $k$ -means-style non-parametric classifiers.

**Training Settings.** We analyse the upper bound of different classifiers by utilising *full supervision* (The labels in both  $\mathcal{D}^l$  and  $\mathcal{D}^u$ ), and study the lower bound of different settings using *minimal supervision* (Only the labels in  $\mathcal{D}^l$ ). For both the *full supervision* setting and the *minimal supervision* setting, by default, we only employ a cross-entropy loss on the labelled samples on hand for classification. Note that unless otherwise stated, this is done on detached features, thus representation learning is not affected.

#### 3.2. Why Prototypical Classification?

**Motivation.** While linear classifiers have been a common choice [28, 30] in supervised and semi-supervised learning, prototypical classifiers take a dominant role in deep clustering [6, 9, 37] and generalized category discovery [4, 14]. In this section, we revisit this option by exploring the upper bound and lower bound of different classifiers with different levels of supervision.

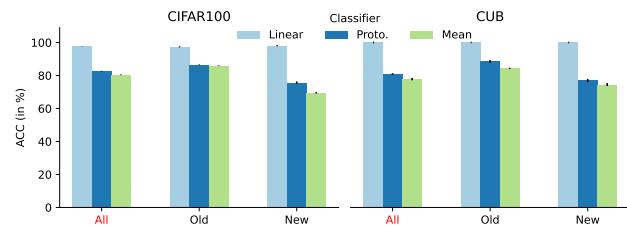


Figure 3. **Results on the upper bound of different classifiers.** In this setting, all labels are available. While the linear classifier conquers this setting, the prototypical classifier still outperforms the mean classifier (upper bound of  $k$ -means). Since all samples are labelled, the difference between ‘Old’ and ‘New’ classes is meaningless, and please refer to the ‘All’ result.

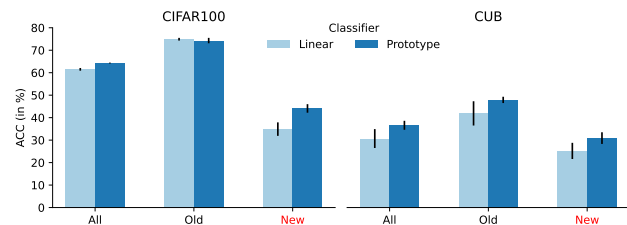


Figure 4. **Results on the lower bound of different classifiers.** In this setting, only labels from old classes are available. While the linear classifier is more biased towards old classes, the prototypical classifier shows better performance on new classes.

**Result & Discussion.** In Fig. 3, we show the results with full supervision and explore the upper bound of different classifiers. In this case, the linear classifier easily approaches 100% accuracy on both datasets, which is expected because of the full supervision, and the linear classifier has more flexibility to adjust its parameters without imposing any regularisation as the prototypical classifier

does. However, if imposing minimal supervision (Fig. 4) with only labelled data  $\mathcal{D}^l$ , it does not show as strong performance on new classes as the prototypical classifier. One explanation is that normalisation helps overcome the optimisation bias toward old categories. In our further experiments combined with self-labelling techniques for the unlabelled samples, instability in optimisation is commonly observed for the linear classifier, mainly due to its nature that the norms of the logits are not bounded. Therefore, we endorse the trend of prototypical classification.

**Takeaway Message.** Though linear classifiers have a higher upper bound if full supervision is available, prototypical classifiers are more favoured since they can better recognise new categories with minimal supervision thanks to the natural logit calibration from feature normalisation.

### 3.3. Which Representation to Build Your Classifier?

**Motivation.** Following the trend of deep clustering that focuses on self-supervised representation learning [6], previous parametric classification work UNO [14] fed the classifier with representations taken from the *projector*. While in GCD [33], significantly stronger performance is achieved with a non-parametric classifier built upon representations taken from the *backbone*. We revisit this choice as follows.

**Setting.** Consider  $f$  as the feature backbone, and  $g$  is a multi-layer perceptron (MLP) projection head. Given an input image  $x_i$ , the representation from the *backbone* can be written as  $f(x_i)$ , and that from the *projector* is  $g(f(x_i))$ . We train a prototypical classifier under the full supervision setting with either representation.

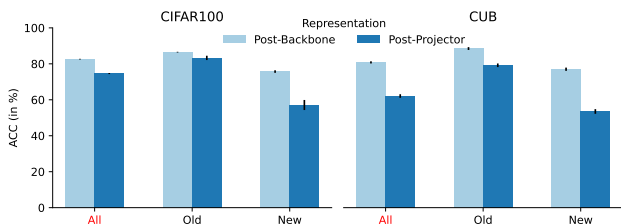


Figure 5. **Results on classification upper bound with different representations.**<sup>1</sup> We adopt a prototypical classifier built on either post-backbone or post-projector representations, and train with full supervision. Given detached representations, those taken from the backbone have a significantly higher upper bound.

**Result & Discussion.** As shown in Fig. 5, the post-backbone feature space has a significantly higher upper bound for learning prototypical classifiers than the post-projector feature space. The use of a projector in self-supervised learning lets the projector focus on solving pretext tasks and allows the backbone to keep as much informa-

<sup>1</sup>The larger gap in ‘New’ classes is a result of GCD [33]’s default sampling strategy, and only the full supervision setting is affected. Please refer to the ‘All’ results since the ‘Old’-‘New’ split is meaningless in this setting.

tion as possible (which facilitates downstream tasks) [10]. However, when good classification performance is all you need, our results suggest that the classification objective should build on post-backbone representations directly before the projector. The features after the projector might focus more on solving the pretext task, which might not be necessarily useful for the classification objective.

**Takeaway Message.** The post-backbone feature space, which is not directly optimised for the pretext task, is favourable for the classification objective than the post-projector feature space.

### 3.4. Decoupled or Joint Representation Learning?

**Motivation.** Previous parametric classification methods, e.g., UNO [14], commonly tune the representations jointly with the classification objective. However, in the non-parametric method GCD [33] where the performance in new classes is notably higher, the representations can be viewed as unaltered by classification when forming the classifier. In this part, we discuss how the classification performance would change if we allow the backbone to be jointly optimised with the classification objective, and explore whether the *joint* learning strategy contributes to previous parametric classifiers’ degraded performance in new classes.

**Setting.** Consider  $f(x)$  as the representation fed to the classifier, *decoupled* training, as the previous settings adopted, indicates  $f(x)$  is detached when computing the logits  $l$ , thus the classification objective won’t supervise representation learning. While for *joint* training, the representations are not detached. We train a prototypical classifier under the minimal supervision setting with either the *decoupled* or *joint* training paradigm. If *w/o self-label*, as before, we do not utilise the unlabelled samples; and if *w/ self-label*, we predict the pseudo-labels for the unlabelled samples with the Sinkhorn Knopp algorithm following [14]. Further, we evaluate the setting *w/ self-distill*, which depicts another pseudo-labelling strategy as in Fig. 7 and will be introduced in detail in Sec. 4.2.

**Result & Discussion.** The results are illustrated in Fig. 6. When only the ground-truth labels (which are absolutely correct) on hand are utilised, for both datasets, jointly supervising the representation with classifier learning can improve the performance on new categories (1% for CIFAR100 and 5% for CUB), while the results of old classes can drop by a relatively small margin. This is acceptable since we care more about new classes. However, if we also adopt the pseudo-labels (which can be unreliable) produced online for the unlabelled samples, there is a sharp drop in old-class performance on both datasets, while for the new classes, it can improve by 13 points on CIFAR100, and drop by a small margin on CUB. This means that *the joint training strategy does not necessarily result in UNO [14]’s low*

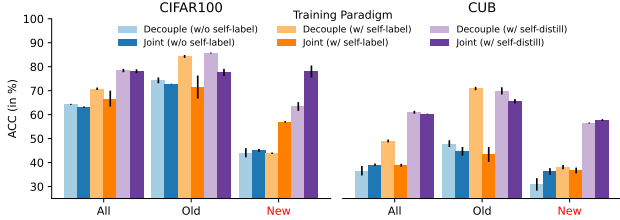


Figure 6. **Results with or without joint training.** We adopt the minimal supervision setting and train a prototypical classifier with only labelled samples (*w/o self-label*) or also utilise the unlabelled samples by either self-labelling (*w/ self-label*, UNO [14]-style) or self-distillation (*w/ self-distill*, as in Fig. 7). *Decouple* denotes the classifier adopts detached features, while *Joint* indicates the classification objective can affect representation learning.

*performance in new classes*; on the contrary, it can even boost new class performance by a notable margin.

Empirically, we then evaluated another pseudo-labelling paradigm: self-distillation. We leave the details in Sec. 4.2, and to put it shortly, this paradigm gains better from joint training, resulting in higher gains in new classes, while significantly less drop in old classes. Our overall explanation is that one of the key factors of UNO’s degraded performance in new classes is its pseudo-labelling strategy could not make reliable predictions. The joint training strategy is not to blame and is, in fact, helpful. When switching to a more advanced pseudo-labelling paradigm that produces higher-quality pseudo-labels, the help from joint training can be even more significant.

**Takeaway Message.** Jointly supervising the representation with a classification objective is helpful for parametric classifiers to recognise new classes. One key factor to blame in previous parametric methods is the paradigm for producing pseudo-labels, and when equipped with a more advanced one, the help from joint training can be even bigger.

## 4. Method

In this section, we present the whole picture of this simple yet effective method (see Fig. 7). And in Sec. 5.3, we discuss the step-by-step changes that lead a simple baseline to our design for generalized category discovery.

### 4.1. Representation Learning

Our representation learning objective follows GCD [33], which is supervised contrastive learning [21] on labelled samples, and self-supervised contrastive learning [8] on all samples. Formally, given two views (random augmentations)  $\mathbf{x}_i$ , and  $\mathbf{x}'_i$  of the same image in a mini-batch  $B$ , the self-supervised contrastive loss is written as:

$$\mathcal{L}_{\text{rep}}^u = \frac{1}{|B|} \sum_{i \in B} -\log \frac{\exp(\mathbf{z}_i^\top \mathbf{z}'_i / \tau_u)}{\sum_{i \neq n} \exp(\mathbf{z}_i^\top \mathbf{z}'_n / \tau_u)}, \quad (1)$$

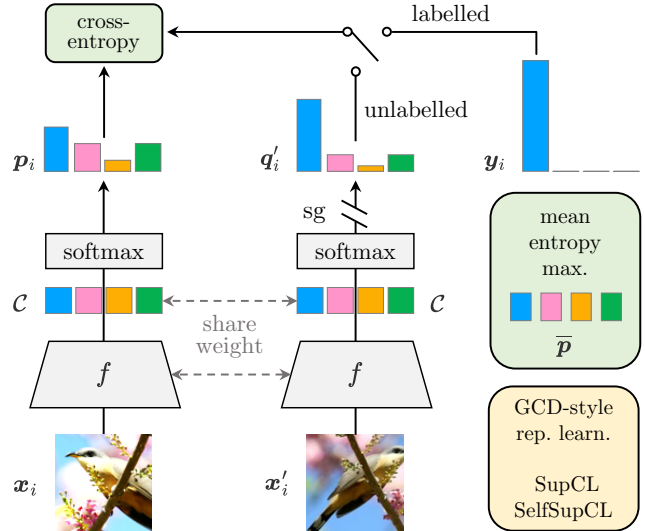


Figure 7. The overall framework of our method. For unlabelled sampled, the soft pseudo-labels are given by sharpened predictions of another random augmented view. And for labelled samples, we simply adopt its ground-truth label. Details for representation learning and the mean-entropy maximisation regulariser are omitted for simplicity, and please refer to the text.

where the feature  $\mathbf{z}_i = g(f(\mathbf{x}_i))$  and is  $\ell_2$ -normalised,  $f, g$  denote the backbone and the projection head, and  $\tau_u$  is a temperature value. The supervised contrastive loss is similar, and the major difference is that positive samples are matched by their labels, formally written as:

$$\mathcal{L}_{\text{rep}}^s = \frac{1}{|B^l|} \sum_{i \in B^l} \frac{1}{|\mathcal{N}_i|} \sum_{q \in \mathcal{N}_i} -\log \frac{\exp(\mathbf{z}_i^\top \mathbf{z}'_q / \tau_c)}{\sum_{i \neq n} \exp(\mathbf{z}_i^\top \mathbf{z}'_n / \tau_c)}, \quad (2)$$

where  $\mathcal{N}_i$  indexes all other images in the same batch that hold the same label as  $\mathbf{x}_i$ . The overall representation learning loss is balanced with  $\lambda$ :

$$\mathcal{L}_{\text{rep}} = (1 - \lambda) \mathcal{L}_{\text{rep}}^u + \lambda \mathcal{L}_{\text{rep}}^s, \quad (3)$$

where  $B^l$  corresponds to the labelled subset of  $B$ .

### 4.2. Parametric Classification

Our parametric classification paradigm follows the self-distillation [1, 7] fashion. Formally, with  $K = |\mathcal{Y}_l \cup \mathcal{Y}_u|$  denoting the total number of categories, we randomly initialise a set of prototypes  $\mathcal{C} = \{\mathbf{c}_1, \dots, \mathbf{c}_K\}$ , each standing for the prototype of one category. During training, for each augmented view  $\mathbf{x}_i$ , we calculate its soft class prediction by softmax on cosine similarity between the hidden feature  $\mathbf{h}_i = f(\mathbf{x}_i)$  and the prototypes  $\mathcal{C}$  scaled by  $1/\tau_s$ :

$$\mathbf{p}_i^{(k)} = \frac{\exp\left(\frac{1}{\tau_s} (\mathbf{h}_i / \|\mathbf{h}_i\|_2)^\top (\mathbf{c}_k / \|\mathbf{c}_k\|_2)\right)}{\sum_{k'} \exp\left(\frac{1}{\tau_s} (\mathbf{h}_i / \|\mathbf{h}_i\|_2)^\top (\mathbf{c}_{k'} / \|\mathbf{c}_{k'}\|_2)\right)}, \quad (4)$$

and the soft pseudo-label  $q'_i$  is produced by another view  $x_i$  with a sharper temperature  $\tau_t$  in a similar fashion. The classification objectives are then simply cross-entropy loss  $\ell(q', p) = -\sum_k q'^{(k)} \log p^{(k)}$  between the predictions and pseudo-labels or ground-truth labels:

$$\mathcal{L}_{\text{cls}}^u = \frac{1}{|B|} \sum_{i \in B} \ell(q'_i, p_i) + \varepsilon H(\bar{p}), \mathcal{L}_{\text{cls}}^s = \frac{1}{|B^l|} \sum_{i \in B^l} \ell(y_i, p_i), \quad (5)$$

where  $y_i$  denote the one-hot label of  $x_i$ . We also adopt a mean-entropy maximisation regulariser [1] for the unsupervised objective. Here  $\bar{p} = \frac{1}{2|B|} \sum_{i \in B} (p_i + p'_i)$  denotes the mean prediction of a batch, and the entropy  $H(\bar{p}) = -\sum_k \bar{p}^{(k)} \log \bar{p}^{(k)}$ . As we will show in Secs. 5.3 and 5.4, this term helps calibrate the predictions’ class distribution and avoid the presence of “dead” prototypes (to which only one or even none of the samples is assigned), which is commonly observed in previous works [33, 37].

Then the classification objective is  $\mathcal{L}_{\text{cls}} = (1 - \lambda)\mathcal{L}_{\text{cls}}^u + \lambda\mathcal{L}_{\text{cls}}^s$  and the overall objective is simply  $\mathcal{L}_{\text{rep}} + \mathcal{L}_{\text{cls}}$ .

**Discussions.** It should be clarified that this work doesn’t aim to promote new methods but to examine existing solutions, provide insights on their failures and build a simple yet strong baseline. The philosophy of producing pseudo-labels from sharpened predictions of another augmented view appears to resemble consistency-based methods [3, 28, 30] in the SSL community. However, despite differences in augmentation strategies and soft/hard pseudo-labels, our approach jointly performs category discovery and self-training style learning, while the SSL methods purely focus on bootstrapping itself with unlabelled data, and does not discover novel categories.

## 5. Experiments

### 5.1. Experimental Setup

**Datasets.** We validate the effectiveness of our method on the generic image recognition benchmark (including CIFAR10/100 [23] and ImageNet-100 [31]), the recently proposed Semantic Shift Benchmark [34] (SSB, including CUB [35], Stanford Cars [22], and FGVC-Aircraft [25]), and also Herbarium 19 [29]. For each dataset, we follow [33] to sample a subset of all classes as the old classes  $\mathcal{Y}_l$ ; 50% of the images from these labelled classes are used to construct  $\mathcal{D}^l$ , and the remaining images are regarded as the unlabelled data  $\mathcal{D}^u$ . See Tab. 1 for statistics of the datasets we evaluate on.

**Evaluation Protocol.** We evaluate the model performance with clustering accuracy (ACC) following standard practice [33]. During evaluation, given the ground truth  $y^*$  and the predicted labels  $\hat{y}$ , the ACC is calculated as  $\text{ACC} = \frac{1}{M} \sum_{i=1}^M \mathbb{1}(y_i^* = p(\hat{y}_i))$  where  $M = |\mathcal{D}^u|$ , and  $p$  is the

Dataset	Balance	Labelled		Unlabelled	
		#Image	#Class	#Image	#Class
CIFAR10 [23]	✓	12.5K	5	37.5K	10
CIFAR100 [23]	✓	20.0K	80	30.0K	100
ImageNet-100 [31]	✓	31.9K	50	95.3K	100
CUB [35]	✓	1.5K	100	4.5K	200
Stanford Cars [22]	✓	2.0K	98	6.1K	196
FGVC-Aircraft [25]	✓	1.7K	50	5.0K	50
Herbarium 19 [29]	✗	8.9K	341	25.4K	683

Table 1. Statistics of the datasets we evaluate on.

optimal permutation that matches the predicted cluster assignments to the ground truth class labels. Besides, since the split for evaluation of Herbarium 19 is imbalanced, we also report the balanced ACC (calculated as the average of per-class ACCs) to avoid biased evaluation.

**Implementation Details.** Following GCD [33], we train all methods with a ViT-B/16 backbone [12] pre-trained with DINO [7]. We use the output of [CLS] token with a dimension of 768 as the feature for an image, and only fine-tune the last block of the backbone. We train with a batch size of 128, and an initial learning rate of 0.1 decayed with a cosine schedule. For a fair comparison, we train for 200 epochs on each dataset, and the best-performing model is selected using the accuracy on the validation set of the labelled classes. Aligning with [33], the balancing factor  $\lambda$  is set to 0.35, and the temperature values  $\tau_u, \tau_c$  as 0.07, 1.0, respectively. For the classification objective, we set  $\tau_s$  to 0.1, and  $\tau_t$  is initialised to 0.07, then warmed up to 0.04 with a cosine schedule in the starting 30 epochs. Besides, the weight  $\varepsilon$  of the regulariser is set to 2. All experiments are done with an NVIDIA GeForce RTX 3090 GPU.

### 5.2. Comparison with the State of the Arts

We compare with state-of-the-art methods in generalized category discovery (ORCA [4] and GCD [33]), strong baselines derived from novel category discovery (RankStats+ [17] and UNO+ [14]), and direct  $k$ -means [24] on DINO [7] features. On both the generic image recognition datasets (Tab. 2a) and the harder SSB benchmark (Tab. 2b), our method achieves notable improvements in recognising new classes (across the instances in  $\mathcal{D}^u$  that belong to classes in  $\mathcal{Y}_u \setminus \mathcal{Y}_l$ ), outperforming the SOTAs by around 10%. The results in old classes are relatively lower, yet they are still competitive against the best-performing baselines. Given that the ability to discover new classes is a more desirable ability, the results are quite encouraging.

In Tab. 3, we also report the results on Herbarium 19 [29], a naturally long-tailed fine-grained dataset that is closer to the real-world application of generalized category discovery. One concern is that its test split is also long-tailed, which may conceal the bias of models. Thus we also report the balanced ACC, which is simply the average of per-class vanilla ACCs and avoids the imbalance between

Methods	CIFAR10			CIFAR100			ImageNet-100		
	All	Old	New	All	Old	New	All	Old	New
<i>k</i> -means [24]	83.6	85.7	82.5	52.0	52.2	50.8	72.7	75.5	<u>71.3</u>
RankStats+ [17]	46.8	19.2	60.5	58.2	<u>77.6</u>	19.3	37.1	61.6	24.8
UNO+ [14]	68.6	<b>98.3</b>	53.8	69.5	<b>80.6</b>	47.2	70.3	<b>95.0</b>	57.9
ORCA [4]	81.8	86.2	79.6	69.0	77.4	52.0	73.5	<u>92.6</u>	63.9
GCD [33]	<u>91.5</u>	<u>97.9</u>	<u>88.2</u>	<u>73.0</u>	<u>76.2</u>	<u>66.5</u>	<u>74.1</u>	89.8	66.3
SimGCD (Ours)	<b>93.2</b> $\pm$ 0.4	82.0 $\pm$ 1.2	<b>98.9</b> $\pm$ 0.0	<b>78.1</b> $\pm$ 0.8	<u>77.6</u> $\pm$ 1.5	<b>78.0</b> $\pm$ 2.5	<b>82.4</b> $\pm$ 0.9	90.7 $\pm$ 0.6	<b>78.3</b> $\pm$ 1.2

(a) Results on generic image recognition datasets.

Methods	CUB			Stanford Cars			FGVC-Aircraft		
	All	Old	New	All	Old	New	All	Old	New
<i>k</i> -means [24]	34.3	38.9	32.1	12.8	10.6	13.8	16.0	14.4	16.8
RankStats+ [17]	33.3	51.6	24.2	28.3	61.8	12.1	26.9	36.4	22.2
UNO+ [14]	35.1	49.0	28.1	35.5	<b>70.5</b>	18.6	40.3	<b>56.4</b>	32.2
ORCA [4]	35.3	45.6	30.2	23.5	50.1	10.7	22.0	31.8	17.1
GCD [33]	<u>51.3</u>	<u>56.6</u>	<u>48.7</u>	<u>39.0</u>	57.6	<u>29.9</u>	<u>45.0</u>	41.1	<u>46.9</u>
SimGCD (Ours)	<b>60.3</b> $\pm$ 0.1	<b>65.6</b> $\pm$ 0.9	<b>57.7</b> $\pm$ 0.4	<b>46.8</b> $\pm$ 1.8	<u>64.9</u> $\pm$ 1.3	<b>38.0</b> $\pm$ 2.1	<b>48.8</b> $\pm$ 2.2	<u>51.0</u> $\pm$ 2.2	<b>47.8</b> $\pm$ 2.7

(b) Results on the Semantic Shift Benchmark [34].

Table 2. Main results. SimGCD achieves significant improvements in recognising new classes. (**bold/under line**: 1<sup>st</sup>/2<sup>nd</sup> performance)

Methods	Vanilla ACC			Balanced ACC		
	All	Old	New	All	Old	New
<i>k</i> -means [24]	13.0	12.2	13.4	13.6	12.2	15.0
RankStats+ [17]	27.9	<u>55.8</u>	12.8	-	-	-
UNO+ [14]	28.3	53.7	14.7	-	-	-
ORCA [4]	20.9	30.9	15.5	9.8	14.7	4.9
GCD [33]	<u>35.4</u>	51.0	<u>27.0</u>	<u>32.8</u>	<u>41.4</u>	<u>24.2</u>
SimGCD (Ours)	<b>43.3</b> $\pm$ 0.3	<b>57.9</b> $\pm$ 0.5	<b>35.3</b> $\pm$ 0.2	<b>39.4</b> $\pm$ 0.4	<b>51.4</b> $\pm$ 1.1	<b>27.3</b> $\pm$ 0.4

Table 3. Results on Herbarium 19 [29].

Methods	CIFAR100			CUB		
	All	Old	New	All	Old	New
(1) UNO+ [14]	69.5	80.6	47.2	35.1	49.0	28.1
(2) + GCD-Style Rep. Learning [33]	67.9	78.9	46.0	45.4	64.2	36.0
(3) + Post-Backbone Representation	70.8	84.3	43.9	49.0	<b>70.9</b>	38.1
(4) + Self-Distill. for Cls. Learning	64.9	73.1	48.2	38.2	44.0	35.3
(5) + ME-Max Regularisation	<b>79.7</b>	<b>86.2</b>	66.6	56.7	67.7	51.3
(6) + Teacher Temp. Warmup	78.4	85.7	63.4	<b>61.0</b>	69.9	56.5
(7) + Joint Training Rep. w/ Cls.	78.1	77.6	<b>78.0</b>	60.3	65.6	<b>57.7</b>

Table 4. Step-by-step ablation study.

classes in the metric. Still, our method shows consistent improvements in all metrics.

In Fig. 2, we compare the time cost for label assignment with GCD [33], one iconic non-parametric classification method. Let the number of all samples and unlabelled samples be  $N$  and  $N_u$ , the number of classes  $K$ , feature dimension  $d$ , and the number of  $k$ -means iterations to be  $t$ , the time complexity of GCD is  $\mathcal{O}(N^2d + NKdt)$  (including  $k$ -means++ initialisation), while our method only requires a nearest-neighbour prototype search for each instance, with time complexity  $\mathcal{O}(N_uKd)$ . All methods adopt GPU implementation and omit the cost for feature extraction.

### 5.3. Ablation Study

In Tab. 4, we ablate the key components that bring the baseline method step-by-step to a new SOTA.

**Baseline.** We start from UNO+ [14], a two-stage parametric classification framework. In the first stage, the backbone is trained with a cross-entropy loss with the labelled samples to learn discriminative features; and in the second stage, it adopts a SwAV [6]-like self-labelling strategy and a classification objective to learn a classifier. The classifier consists of two heads: one for the old classes built on the backbone, and one for the new classes built on the projector. The backbone is jointly tuned in the classifier learning stage.

**Improving the Representations.** In rows (2) and (3), we explore improving the representations of UNO+. We first align its representation learning objective with GCD [33] (see Sec. 4.1). We jointly train this objective with the classification objective in a decoupled manner, thus simplifying the training schedule while maintaining fair comparison. As in row (2), this makes little difference for CIFAR100, but significantly improves CUB in both old classes (5%) and new classes (8%). As suggested in Sec. 3.3, we then sim-

plify the classifier into a single head built on the backbone. As shown in row (3), this makes notable improvements in old classes for both datasets (5%, 7%).

**Improving the Pseudo Labels.** In rows (4), (5), and (6), we explore improving the pseudo-labelling strategy. We start with replacing the Sinkhorn-Knopp algorithm with a vanilla self-distillation paradigm (Eq. (5) with  $\varepsilon = 0$ ). Though this results in a sharp performance drop, when combined with a mean-entropy maximisation regulariser, as in row (5), we achieve consistent improvements over row (3) by a large margin (26% in CIFAR100, 13% in CUB) in new classes. Our intuition is that this regulariser can be viewed as a softened counterpart of the Sinkhorn-Knopp algorithm, and helps calibrate the predictions’ class distribution in a more suitable way. We then further adopt a teacher temperature warmup strategy to lower the confidence of the pseudo-labels at an earlier stage. The intuition is that at the beginning, both the classifier and the representation are not well fitted to the target data, thus the pseudo-labels are not quite reliable. As reported in row (6), this is indeed helpful for CUB, resulting in an improvement of 5% in new classes. While for CIFAR100, which is much similar to the pre-training data (ImageNet), the unreliable pseudo label is not a problem, thus lowering the confidence results in 3 points’ drop in new classes. For simplicity, we keep the training strategy consistent with CUB.

**Jointly Training the Representation.** Previous settings adopt a decoupled training strategy for consistent representations with GCD [33] and fair comparison. Finally, as confirmed in Sec. 3.4, we jointly supervise the representation with the classification objective. As in row (7), this results in a significant improvement in new classes for CIFAR100 (15%), with also a considerable drop in old classes (8%).

The overall gain for CUB is, in contrast, relatively small. We leave the discussions in Sec. 5.4. For simplicity, we keep the training strategy consistent with CIFAR100.

The model used in row (7) is the same as the final model for experimental results and is introduced in detail in Sec. 4.

### 5.4. Discussions

**What Makes for the Significant Improvements Over GCD Given the Same Representations?** One interesting message from row (6) of Tab. 4 is that, even with the same representations, for SSB [34] datasets like CUB, we can already improve GCD overall by 10%. We thus study the classification predictions and the major components that lead to the performance gap. As shown in Fig. 8, the non-parametric classifier (semi-supervised  $k$ -means) adopted by GCD [33] produces highly imbalanced predictions, while our method better fits the true distribution. Further analysis shows that our method significantly improves over the tail classes of GCD. Concerning why this improvement is relatively small on CIFAR100, our intuition is: for generic classification, the number of instances per class is much more abundant, therefore semi-supervised  $k$ -means can be more robust, and our improvement is not as notable.

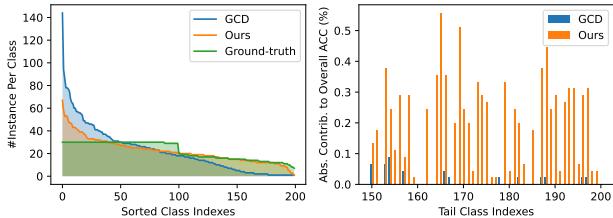


Figure 8. Classification result analysis on CUB [35]. Left: Based on identical representations, the non-parametric classifier (semi-supervised  $k$ -means) adopted by GCD [33] produces highly imbalanced predictions, while our method better fits the true distribution; Right: our method significantly improves GCD’s tail classes.

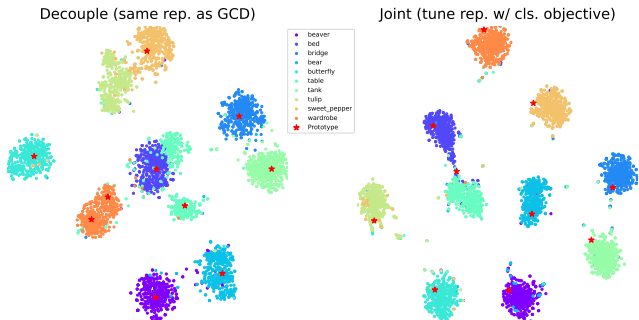


Figure 9. T-SNE [32] visualisation of the representations of 10 classes randomly sampled from CIFAR100 [23]. Jointly supervising representation learning with a classification objective helps disambiguate (*e.g.*, bed & table) and forms compacter clusters.

**How Does the Classification Objective Change the Representations?** In row (7) of Tab. 4, we have shown that

jointly training the representations with the classification objective can lead to  $\sim 15\%$  boost in new classes on CIFAR100. We study this difference by visualising the representations before and after tuning with t-SNE [32]. As illustrated in Fig. 9, jointly tuning the feature leads to less ambiguity, larger margins, and more compact clusters.

Concerning why this is not as helpful for SSB: we hypothesise that one important factor lies in how transferable the features learned in old classes are to novel classes. While it may be easier for a cat classifier to be adapted to dogs, things can be different for fine-grained bird recognition. Besides, the small scale of CUB, which contains only 6k images while holding a fine-grained class split (200), might also make it hard to learn transferrable features.

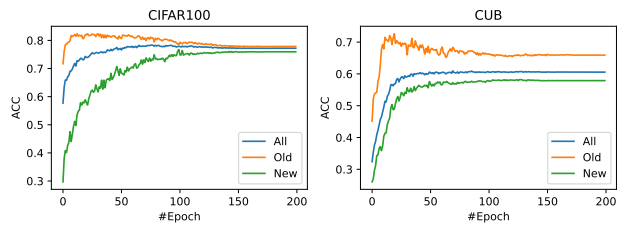


Figure 10. We observe a trade-off between the performance in ‘Old’ and ‘New’ categories, which is common across datasets.

**Trade-off Between Old and New Categories.** We plot the performance evolution throughout the model learning process in Fig. 10. It can be observed that the performance on the ‘Old’ categories first climbs to the highest point at the early stage of training and then slowly degrades as the performance on the ‘New’ categories improves. We believe this demonstrates an important aspect of the design of models for the GCD problem: the performance on the ‘Old’ categories may be in odd with the performance on the ‘New’ categories, how to achieve a better trade-off between these two could be an interesting investigation for future works.

## 6. Conclusion

In this work, we revisit the reason that makes previous parametric classifiers fail to recognise new classes for GCD. Our investigations show that the less discriminative representations and unreliable pseudo-labelling strategy are key factors that make parametric classifiers lag behind non-parametric ones. We then present a simple yet effective parametric classification baseline that outperforms previous SOTAs by a large margin on multiple GCD benchmarks.

## Acknowledgements

This work has been supported by Hong Kong Research Grant Council - Early Career Scheme (Grant No. 27209621), HKU Startup Fund, and HKU Seed Fund for Basic Research. The authors acknowledge SmartMore and MEGVII for partial computing support.



## References

- [1] Mahmoud Assran, Mathilde Caron, Ishan Misra, Piotr Bojanowski, Florian Bordes, Pascal Vincent, Armand Joulin, Mike Rabbat, and Nicolas Ballas. Masked siamese networks for label-efficient learning. In *ECCV*, 2022. 2, 3, 5, 6
- [2] Mahmoud Assran, Mathilde Caron, Ishan Misra, Piotr Bojanowski, Armand Joulin, Nicolas Ballas, and Michael Rabbat. Semi-supervised learning of visual features by non-parametrically predicting view assignments with support samples. In *ICCV*, 2021. 3
- [3] David Berthelot, Nicholas Carlini, Ian Goodfellow, Nicolas Papernot, Avital Oliver, and Colin Raffel. Mixmatch: A holistic approach to semi-supervised learning. In *NeurIPS*, 2019. 1, 2, 6
- [4] Kaidi Cao, Maria Brbić, and Jure Leskovec. Open-world semi-supervised learning. In *ICLR*, 2022. 1, 2, 3, 6, 7
- [5] Mathilde Caron, Piotr Bojanowski, Armand Joulin, and Matthijs Douze. Deep Clustering for Unsupervised Learning of Visual Features. In *ECCV*, 2018. 2, 3
- [6] Mathilde Caron, Ishan Misra, Julien Mairal, Priya Goyal, Piotr Bojanowski, and Armand Joulin. Unsupervised learning of visual features by contrasting cluster assignments. In *nips*, 2020. 2, 3, 4, 7, 13
- [7] Mathilde Caron, Hugo Touvron, Ishan Misra, Hervé Jégou, Julien Mairal, Piotr Bojanowski, and Armand Joulin. Emerging properties in self-supervised vision transformers. In *ICCV*, 2021. 2, 3, 5, 6
- [8] Ting Chen, Simon Kornblith, Mohammad Norouzi, and Geoffrey Hinton. A simple framework for contrastive learning of visual representations. In *ICML*, 2020. 3, 5, 13
- [9] Jang Hyun Cho, Utkarsh Mall, Kavita Bala, and Bharath Hariharan. Picie: Unsupervised semantic segmentation using invariance and equivariance in clustering. In *CVPR*, 2021. 3
- [10] Quan Cui, Bingchen Zhao, Zhao-Min Chen, Borui Zhao, Renjie Song, Jiajun Liang, Boyan Zhou, and Osamu Yoshie. Discriminability-transferability trade-off: An information-theoretic perspective. In *ECCV*, 2022. 4
- [11] Jia Deng, Wei Dong, Richard Socher, Li-Jia Li, Kai Li, and Li Fei-Fei. Imagenet: A large-scale hierarchical image database. In *CVPR*, 2009. 12
- [12] Alexey Dosovitskiy, Lucas Beyer, Alexander Kolesnikov, Dirk Weissenborn, Xiaohua Zhai, Thomas Unterthiner, Mostafa Dehghani, Matthias Minderer, Georg Heigold, Sylvain Gelly, Jakob Uszkoreit, and Neil Houlsby. An image is worth 16x16 words: Transformers for image recognition at scale. In *ICLR*, 2021. 6
- [13] Yixin Fei, Zhongkai Zhao, Siwei Yang, and Bingchen Zhao. Xcon: Learning with experts for fine-grained category discovery. In *BMVC*, 2022. 2
- [14] Enrico Fini, Enver Sangineto, Stéphane Lathuilière, Zhun Zhong, Moin Nabi, and Elisa Ricci. A unified objective for novel class discovery. In *ICCV*, 2021. 1, 2, 3, 4, 5, 6, 7, 11, 12, 13
- [15] Spyros Gidaris, Praveer Singh, and Nikos Komodakis. Unsupervised representation learning by predicting image rotations. In *ICLR*, 2018. 2
- [16] Jean-Bastien Grill, Florian Strub, Florent Alché, Corentin Tallec, Pierre Richemond, Elena Buchatskaya, Carl Doersch, Bernardo Avila Pires, Zhaohan Guo, Mohammad Gheshlaghi Azar, et al. Bootstrap your own latent-a new approach to self-supervised learning. In *NeurIPS*, 2020. 13
- [17] Kai Han, Sylvestre-Alvise Rebuffi, Sebastien Ehrhardt, Andrea Vedaldi, and Andrew Zisserman. Autonovel: Automatically discovering and learning novel visual categories. *IEEE TPAMI*, 2021. 1, 2, 3, 6, 7, 12, 13
- [18] Kai Han, Andrea Vedaldi, and Andrew Zisserman. Learning to discover novel visual categories via deep transfer clustering. In *ICCV*, 2019. 2, 3, 13
- [19] Kaiming He, Haoqi Fan, Yuxin Wu, Saining Xie, and Ross Girshick. Momentum contrast for unsupervised visual representation learning. In *CVPR*, 2020. 2
- [20] Kaiming He, Xiangyu Zhang, Shaoqing Ren, and Jian Sun. Deep residual learning for image recognition. In *CVPR*, 2016. 1
- [21] Prannay Khosla, Piotr Teterwak, Chen Wang, Aaron Sarna, Yonglong Tian, Phillip Isola, Aaron Maschiot, Ce Liu, and Dilip Krishnan. Supervised contrastive learning. In *NeurIPS*, 2020. 3, 5
- [22] Jonathan Krause, Michael Stark, Jia Deng, and Li Fei-Fei. 3d object representations for fine-grained categorization. In *4th International IEEE Workshop on 3D Representation and Recognition (3dRR-13)*, 2013. 6, 12
- [23] Alex Krizhevsky and Geoffrey Hinton. Learning multiple layers of features from tiny images. *Technical Report*, 2009. 2, 6, 8, 11, 12
- [24] James MacQueen. Some methods for classification and analysis of multivariate observations. In *Proceedings of the Fifth Berkeley Symposium on Mathematical Statistics and Probability*, 1967. 6, 7
- [25] Subhransu Maji, Esa Rahtu, Juho Kannala, Matthew Blaschko, and Andrea Vedaldi. Fine-grained visual classification of aircraft. *arXiv preprint arXiv:1306.5151*, 2013. 6
- [26] Avital Oliver, Augustus Odena, Colin Raffel, Ekin D Cubuk, and Ian J Goodfellow. Realistic evaluation of deep semi-supervised learning algorithms. In *NeurIPS*, 2018. 1, 2
- [27] Sylvestre-Alvise Rebuffi, Sebastien Ehrhardt, Kai Han, Andrea Vedaldi, and Andrew Zisserman. Semi-supervised learning with scarce annotations. In *CVPR Deep-Vision workshop*, 2020. 2
- [28] Kihyuk Sohn, David Berthelot, Chun-Liang Li, Zizhao Zhang, Nicholas Carlini, Ekin D Cubuk, Alex Kurakin, Han Zhang, and Colin Raffel. Fixmatch: Simplifying semi-supervised learning with consistency and confidence. In *NeurIPS*, 2020. 1, 2, 3, 6
- [29] Kiat Chuan Tan, Yulong Liu, Barbara Ambrose, Melissa Tulig, and Serge Belongie. The herbarium challenge 2019 dataset. In *Workshop on Fine-Grained Visual Categorization*, 2019. 2, 6, 7
- [30] Antti Tarvainen and Harri Valpola. Mean teachers are better role models: Weight-averaged consistency targets improve semi-supervised deep learning results. In *NeurIPS*, 2017. 2, 3, 6

- [31] Yonglong Tian, Dilip Krishnan, and Phillip Isola. Contrastive multiview coding. In *ECCV*, 2020. 6
- [32] Laurens Van der Maaten and Geoffrey Hinton. Visualizing data using t-sne. *JMLR*, 2008. 8
- [33] Sagar Vaze, Kai Han, Andrea Vedaldi, and Andrew Zisserman. Generalized category discovery. In *CVPR*, 2022. 1, 2, 3, 4, 5, 6, 7, 8, 11, 12, 13
- [34] Sagar Vaze, Kai Han, Andrea Vedaldi, and Andrew Zisserman. Open-set recognition: A good closed-set classifier is all you need? In *ICLR*, 2022. 2, 6, 7, 8, 12, 13
- [35] Catherine Wah, Steve Branson, Peter Welinder, Pietro Perona, and Serge Belongie. Caltech-UCSD Birds 200. *Computation & Neural Systems Technical Report*, 2010. 6, 8, 11, 12
- [36] Feng Wang, Xiang Xiang, Jian Cheng, and Alan Loddon Yuille. Normface: L2 hypersphere embedding for face verification. In *ACM MM*, 2017. 3
- [37] Xin Wen, Bingchen Zhao, Anlin Zheng, Xiangyu Zhang, and Xiaojuan Qi. Self-supervised visual representation learning with semantic grouping. In *NeurIPS*, 2022. 3, 6
- [38] Asano Ym, Rupprecht C, and Vedaldi A. Self-labelling via simultaneous clustering and representation learning. In *ICLR*, 2019. 2, 3
- [39] Xiaohua Zhai, Avital Oliver, Alexander Kolesnikov, and Lucas Beyer. S4l: Self-supervised semi-supervised learning. In *ICCV*, 2019. 2
- [40] Bingchen Zhao and Kai Han. Novel visual category discovery with dual ranking statistics and mutual knowledge distillation. In *NeurIPS*, 2021. 2, 3, 12, 13
- [41] Bingchen Zhao and Xin Wen. Distilling visual priors from self-supervised learning. In *ECCV VIPriors Workshop*, 2020. 2
- [42] Zhun Zhong, Enrico Fini, Subhankar Roy, Zhiming Luo, Elisa Ricci, and Nicu Sebe. Neighborhood contrastive learning for novel class discovery. In *CVPR*, 2021. 2
- [43] Zhun Zhong, Linchao Zhu, Zhiming Luo, Shaozi Li, Yi Yang, and Nicu Sebe. Openmix: Reviving known knowledge for discovering novel visual categories in an open world. In *CVPR*, 2021. 2, 3, 12, 13

# A Simple Parametric Classification Baseline for Generalized Category Discovery

## Appendix

Method	All	Old	New	All	Old	New
Self-Label	66.7 $\pm$ 3.3	71.5 $\pm$ 4.8	57.0 $\pm$ 0.3	38.9 $\pm$ 0.6	43.4 $\pm$ 3.1	36.7 $\pm$ 1.2
Self-Distill	<b>78.1<math>\pm</math>0.8</b>	<b>77.6<math>\pm</math>1.5</b>	<b>78.0<math>\pm</math>2.5</b>	<b>60.3<math>\pm</math>0.1</b>	<b>65.6<math>\pm</math>0.9</b>	<b>57.7<math>\pm</math>0.4</b>

(a) Pseudo-labelling strategy (CIFAR100 & CUB)

Paradigm	All	Old	New	All	Old	New
Decouple	<b>78.4<math>\pm</math>0.7</b>	<b>85.7<math>\pm</math>0.2</b>	63.4 $\pm$ 1.8	<b>61.0<math>\pm</math>0.6</b>	<b>69.9<math>\pm</math>1.5</b>	56.5 $\pm$ 0.2
Joint	78.1 $\pm$ 0.8	77.6 $\pm$ 1.5	<b>78.0<math>\pm</math>2.5</b>	60.3 $\pm$ 0.1	65.6 $\pm$ 0.9	<b>57.7<math>\pm</math>0.4</b>

(b) Learning paradigm (CIFAR100 & CUB)

Schedule	All	Old	New	All	Old	New
0.04	<b>79.2<math>\pm</math>0.8</b>	<b>78.8<math>\pm</math>0.4</b>	<b>80.1<math>\pm</math>3.0</b>	45.1 $\pm$ 1.1	58.9 $\pm$ 4.2	43.3 $\pm$ 0.5
0.07	66.2 $\pm$ 1.7	71.7 $\pm$ 1.7	55.3 $\pm$ 1.9	45.7 $\pm$ 1.8	60.9 $\pm$ 4.6	38.1 $\pm$ 0.9
0.07 $\rightarrow$ 0.04	78.1 $\pm$ 0.8	77.6 $\pm$ 1.5	78.0 $\pm$ 2.5	<b>60.3<math>\pm</math>0.1</b>	<b>65.6<math>\pm</math>0.9</b>	<b>57.7<math>\pm</math>0.4</b>

(d) Teacher temperature schedule (CIFAR100 & CUB)

Representation	All	Old	New	All	Old	New
Post-Backbone	78.1 $\pm$ 0.8	<b>77.6<math>\pm</math>1.5</b>	78.0 $\pm$ 2.5	<b>60.3<math>\pm</math>0.1</b>	<b>65.6<math>\pm</math>0.9</b>	<b>57.7<math>\pm</math>0.4</b>
Post-Projector	<b>79.4<math>\pm</math>0.1</b>	77.1 $\pm$ 0.2	<b>83.8<math>\pm</math>0.7</b>	48.7 $\pm$ 1.2	46.0 $\pm$ 2.0	50.1 $\pm$ 0.7

(c) Representation for the classifier (CIFAR100 & CUB)

Weight	All	Old	New	All	Old	New
0	66.4 $\pm$ 0.5	71.8 $\pm$ 0.2	55.5 $\pm$ 1.1	39.7 $\pm$ 0.3	45.1 $\pm$ 1.3	37.0 $\pm$ 0.7
1	77.9 $\pm$ 0.7	<b>83.5<math>\pm</math>0.3</b>	66.7 $\pm$ 1.6	53.8 $\pm$ 1.3	61.6 $\pm$ 1.9	49.9 $\pm$ 1.4
2	78.1 $\pm$ 0.8	77.6 $\pm$ 1.5	<b>78.0<math>\pm</math>2.5</b>	<b>60.3<math>\pm</math>0.1</b>	<b>65.6<math>\pm</math>0.9</b>	<b>57.7<math>\pm</math>0.4</b>
4	<b>80.1<math>\pm</math>0.9</b>	81.2 $\pm$ 0.4	77.8 $\pm$ 2.0	59.0 $\pm$ 0.7	<b>69.6<math>\pm</math>0.4</b>	53.7 $\pm$ 0.9

(e) ME-Max regulariser weight (CIFAR100 & CUB)

Table 5. Ablations on CIFAR100 [23] and CUB [35] about: (a): Pseudo-labelling strategy; (b): Learning paradigm; (c): Representation for the classifier; (d) Teacher temperature schedule; (e) ME-Max regulariser weight. Default options are marked with a grey background.

### A. Extended Ablation Study

**Pseudo-labelling strategy.** In Tab. 5a, we ablate the pseudo-labelling strategy. Compared with the self-labelling method (Sinkhorn Knopp algorithm) adopted by UNO [14], the self-distillation-style pseudo-labelling strategy shows consistently better results on all metrics. Notably, the gains on new classes of both datasets can reach around 20 points. This indicates that the self-distillation strategy is significantly favourable for generalized category discovery.

**Learning paradigm.** In Tab. 5b, we show the results of different learning paradigms. By jointly supervising the representation with the classification objective, we see a significant improvement in new classes for CIFAR100 (15%), with also a considerable drop in old classes (8%). The overall gain for CUB is, in contrast, relatively small. Discussions on this can be found in the main text.

**Representation for the classifier.** In Tab. 5c, we ablate the effect of different representations. For CUB, taking the post-backbone representations yields consistent improvements (20% on old classes, 7.6% on new classes). While for CIFAR100, the post-projector representations can be helpful for recognising new classes (5.8%). As discussed in

the main text, the features after the projector focus more on solving the pretext task, which can be helpful for the classification objective if the pretext task well fits the criterion for the new classes, *e.g.*, CIFAR100, but not for the fine-grained CUB.

**Teacher temperature schedule.** In Tab. 5d, we show the effect of different teacher temperature schedules. A smaller value indicates sharper pseudo-labels. A warmup strategy that lowers the confidence of the pseudo-labels at early stages results in an improvement of 5% in new classes on CUB. While for CIFAR100, which is much similar to the pre-training data (ImageNet), the unreliable pseudo label is not a problem, thus lowering the confidence results in 3 points’ drop in new classes.

**Mean-entropy maximisation regulariser weight.** Tab. 5e ablates the weight for the mean-entropy maximisation regulariser. A higher weight enforces the mean predictions of a batch to imitate uniform distribution, which resembles the Sinkhorn Knopp algorithm’s hard uniform partition constraint. While a lower weight may result in extremely long-tailed predictions as GCD [33] does. Generally, we found setting the weight to 2 reaches a good balance, and shows the best performance in new classes.

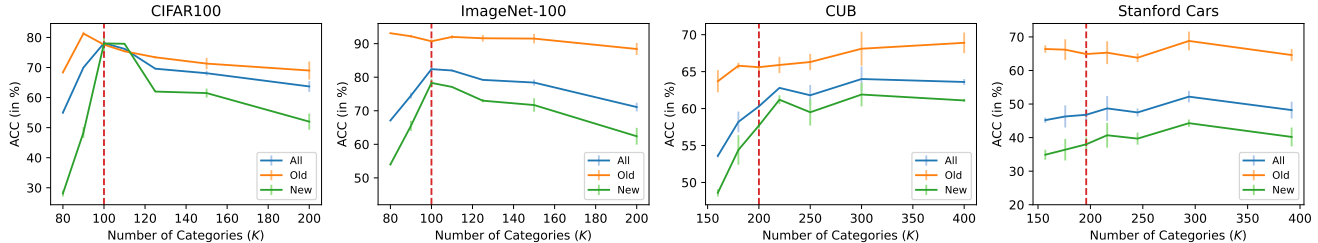


Figure 11. Results with different numbers of categories (dashed red lines indicate the real number of categories). While a category number lower than the ground truth significantly limit the ability to discover new categories, a larger number of categories is less harmful and can even be helpful for the fine-grained SSB datasets.

## B. Unknown Number of Categories

In the main text, we assumed the number of categories is known *a-priori* following prior works [14, 17, 40, 43]. In this section, we report the results with the number of categories estimated using an off-the-shelf method [33] (Tab. 6). Since the estimated  $K$  is identical to the real  $K$  for CIFAR100, we omit the results on it. The results on CIFAR10 [23], ImageNet-100 [11], CUB [35], and Stanford Cars [22] are available in Tabs. 7 and 8.

	CIFAR10	CIFAR100	ImageNet-100	CUB	SCars
Real $K$	10	100	100	200	196
Est. $K$	9	100	109	231	230

Table 6. Number of categories  $K$  estimated using [33].

Methods	Known $K$	CIFAR10			ImageNet-100		
		All	Old	New	All	Old	New
GCD [33]	✓	91.5	<b>97.9</b>	88.2	74.1	89.8	66.3
SimGCD (Ours)	✓	<b>93.2</b>	82.0	<b>98.9</b>	<b>82.4</b>	<b>90.7</b>	<b>78.3</b>
GCD [33]	✗	<b>88.6</b>	<b>96.2</b>	<b>84.9</b>	72.7	<b>91.8</b>	63.8
SimGCD (Ours)	✗	82.8	93.9	77.2	<b>81.5</b>	89.7	<b>77.5</b>

Table 7. Results on generic image recognition datasets.

Methods	Known $K$	CUB			Stanford Cars		
		All	Old	New	All	Old	New
GCD [33]	✓	51.3	56.6	48.7	39.0	57.6	29.9
SimGCD (Ours)	✓	<b>60.3</b>	<b>65.6</b>	<b>57.7</b>	<b>46.8</b>	<b>64.9</b>	<b>38.0</b>
GCD [33]	✗	47.1	55.1	44.8	35.0	56.0	24.8
SimGCD (Ours)	✗	<b>61.5</b>	<b>66.4</b>	<b>59.1</b>	<b>49.1</b>	<b>65.1</b>	<b>41.3</b>

Table 8. Results on the Semantic Shift Benchmark [34].

Generally speaking, if the estimated  $K$  is smaller than the real  $K$ , the model tends to sacrifice the performance of new classes, and focus more on the old classes. On the other hand, if the estimated  $K$  is larger than the real  $K$ , the results are generally robust. Notably, the inaccurate  $K$  estimation

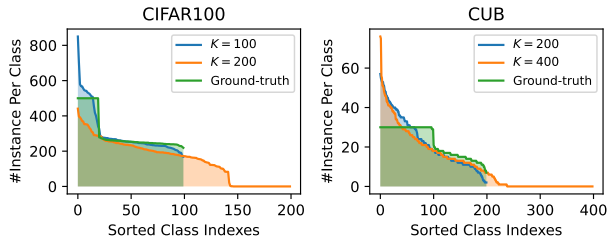


Figure 12. Statistics on the number of instances per class with different numbers of categories. While a larger category number introduces more classes ( $\sim 50\%$ ) to the coarse-grained CIFAR100, it is interesting to see the network prefers to keep the number of active prototypes low and close to the real category number (200) for the fine-grained CUB.

can cause gains  $\sim 3$  points in new classes in CUB and Stanford Cars. This motivates us to further analyse the influence of the estimated category number, detailed as follows.

In Fig. 11, we present the results with different numbers of categories on four representative datasets. A category number lower than the ground truth significantly limits the ability to discover new categories, and the model tends to focus more on the old classes. On the other hand, increasing the number of categories results in less harm to the generic image recognition datasets and can even be helpful for the fine-grained SSB datasets.

Generally speaking, increasing the number of predicted classes can produce more robust prototypes, thus decreasing the number of *false positives* (misclassified instances), and on the other hand, increasing the number of *false negatives* (instances classified into redundant classes). It is interesting to see that on CUB and Stanford Cars, even using  $2\times$  of the real number of categories does not result in a notable performance drop (caused by the increase in false negatives). This motivates us to further investigate the size of different clusters with different category numbers (Fig. 12). While a larger category number introduces more active classes ( $\sim 50\%$ ) to the coarse-grained CIFAR100, it is interesting to see the network prefers to keep the number of active prototypes low and close to the real category number for the fine-grained CUB. This phenomenon might motivate an end-to-end category number estimation method in the future.

## C. Limitations and Potential Future Works

**Representation Learning.** This paper mainly targets improving the classification ability for generalized category discovery. The representation learning, however, follows the prior work GCD [33]. It is expectable that the quality of representation learning can be improved. For instance, generally, by using more advanced geometric and photometric data augmentations [16], and even multiple local crops [6]. Further, can the design of data augmentations be better aligned with the classification criteria of the target data? For another example, a large batch size has been shown to be critical to the performance of contrastive learning-based frameworks [8]. However, the batch size adopted by GCD [33] is only 128, which might limit the quality of learned representations. Moreover, is the supervised contrastive learning plus self-supervised contrastive learning paradigm the ultimate answer to form the feature manifold? We believe that advances in representation learning can lead to further gains.

**Unknown Category Number.** This paper assumes the number of categories is known *a-priori* [14, 17, 40, 43], or can be estimated using off-the-shelf methods [18, 33]. In Figs. 11 and 12, we discovered that even given a large category-number estimation, the model could fit well to the real number of categories on the semantic shift benchmark [34]. We believe that further explorations on this phenomenon might motivate improvements that can allow the model to jointly estimate the number of categories in an end-to-end manner.

**Ethical Considerations.** Current methods commonly suffer from low-data or long-tailed scenarios. Depending on the data and classification criteria of specific tasks, discrimination against minority categories or instances is possible.